On the Stereochemical Outcome of the Catalyzed and Uncatalyzed Cycloaddition Reaction between Activated Ketenes and Aldehydes to form *cis*- and *trans*-2-Oxetanones. An *ab Initio* Study

Begoña Lecea,[†] Ana Arrieta,[‡] Xabier Lopez,[‡] Jesus M. Ugalde,[‡] and Fernando P. Cossío*,[‡]

Contribution from Farmazi Fakultatea, Euskal Herriko Unibertsitatea, P.K. 45 ,01080 Vitoria-Gasteiz, Spain, and Kimika Fakultatea, Euskal Herriko Unibertsitatea, P.K. 1072, 20080 San Sebastián-Donostia, Spain

Received May 30, 1995[⊗]

Abstract: The possible reaction paths corresponding to the catalyzed and uncatalyzed reaction between chloroketene (as a model activated ketene) and acetaldehyde (as a model alkyl carbonyl compound) have been studied using *ab initio* methodologies and taking into account solvent effects. Eight transition structures have been located and characterized, both in the gas phase and in solution. It has been found that formation of *trans*-2-oxetanones is favored in the absence of catalyst, whereas the catalyzed reaction leads to the preferential formation of the corresponding *cis* cycloadducts. These results are in qualitative agreement with the experimental data available.

Introduction

The [2 + 2] cycloaddition between ketenes and carbonyl compounds was discovered by Staudinger[1] in 1911. This reaction has significant synthetic relevance[2] since it provides a convergent entry to 2-oxetanone nuclei (Scheme 1), whose importance as synthetic intermediates or as target molecules is well-known.[2a,3] Some recent relevant examples on active research involving this cycloaddition include an improved total synthesis of (−)-tetrahydrolipstatin,[4] an asymmetric synthesis of either (*R*)- or (*S*)-4-trichloromethyl-2-oxetanone using polymeric chinchona alcaloids as catalysts,[5] synthesis of bicyclic 2-oxetanones by means of intramolecular photochemical reaction of chromium alkoxy carbenes with aldehydes,[6] and asymmetric synthesis of 4-substituted-2-oxetanones catalyzed by C_2 chiral aluminium complexes.[7]

In spite of the practical importance of this reaction, its mechanism was not studied using modern MO-SCF computational tools until 1993.[8] Recently, our group has published a theoretical study on the catalyzed and uncatalyzed reaction between formaldehyde and either ketene and chloroketene to yield 2-oxetanone and 3-chloro-2-oxetanone, respectively,[9] Solvent effects were included in this study. The main conclusions from these papers are that the uncatalyzed reaction between ketenes and carbonyl compounds is a concerted process whose transition structure (TS hereafter) corresponds to a $[_{\pi}2_s+(_{\pi}2_s+_{\pi}2_s)]$ mechanism.[10] By contrast, the catalyzed reaction takes place *via* two-stage TSs in which bonding between C(3) and C(4) is very advanced, whereas the O(1)−C(2) bond order is virtually negligible. These findings have appeared almost simultaneously with a preliminary communication from another group.[11] In this paper, Rajzmann *et al.* (PPRL hereafter) reported a theoretical study on the [2 + 2] cycloaddition between ketene

Scheme 1[a]

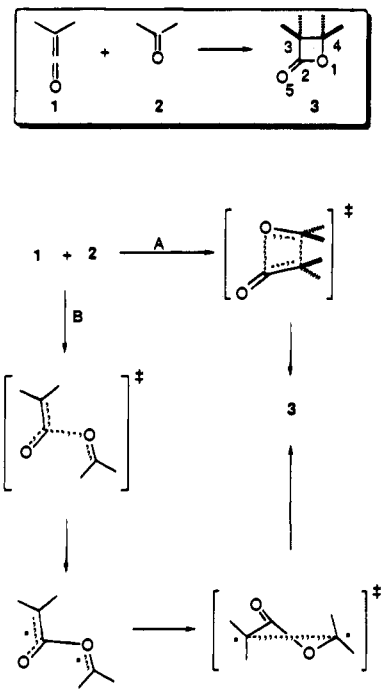

[a] The possible substituents at the different positions are not specified.

[†] Farmazi Fakultatea.

[‡] Kimika Fakultatea.

[⊗] Abstract published in *Advance ACS Abstracts*, November 15, 1995.

(1) Staudinger, H.; Bereza, S. Ann. **1991**, *380*, 243.

(2) (a) Pommier, A.; Pons, J.-M. Synthesis **1993**, 441. (b) Ghosez, L.; Marchand-Brynaert, J. In *Comprehensive Organic Chemistry*; Trost, B. M., Fleming, I., Eds.; Pergamon: Oxford, 1991; Vol. 5, pp 86−89.

(3) See, for example: Danheiser, R. L.; Nowick, J. S. *J. Org. Chem.* **1991**, *56*, 1176 and references therein.

(4) Pommier, A.; Pons, J.-M.; Kocienski, P. J.; Wong, L. *Synthesis* **1994**, 1294.

(5) Song, C. E.; Ryu, T. H. R.; Roh, E. J.; Kim, I. O.; Ha, H.-J. *Tetrahedron:Asymmetry* **1994**, *5*, 1215.

(6) Colson, J.-P.; Hegedus, L. S. *J. Org. Chem.* **1994**, *59*, 4972.

(7) (a) Tamai, Y.; Yoshiwara, H.; Someya, M.; Fukumoto, J.; Miyano, S. *J. Chem. Soc., Chem. Commun.* **1994**, 2281. (b) Tamai, Y.; Someya, M.; Fukumoto, J.; Miyano, S. *J. Chem. Soc., Perkin Trans. 1* **1994**, 1549.

(8) Yamabe, S.; Minato, T.; Osamura, Y. *J. Chem. Soc., Chem. Commun.* **1993**, 450.

(9) Lecea, B.; Arrieta, A.; Roa, G.; Ugalde, J. M.; Cossío, F. P. *J. Am. Chem. Soc.* **1994**, *116*, 9613.

(10) (a) Pasto, D. J. *J. Am. Chem. Soc.* **1979**, *101*, 37. (b) Krabbenhoft, H. O. *J. Org. Chem.* **1978**, *43*, 1305.

0002-7863/95/1517-12314$09.00/0

Scheme 2

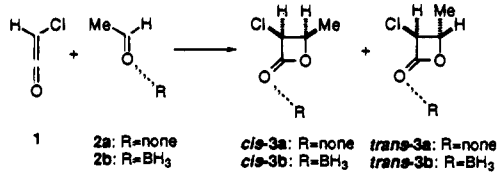

and formaldehyde to form 2-oxetanone, using the semiempirical hamiltonian AM1[12] at a configuration interaction-half electron[13] (CI-HE) level of theory, PPRL considered two alternative pathways: a concerted mechanism in which bonding between C(3) and C(4) should be more advanced than that between O(1) and C(2) (mechanism **A**, Scheme 1) and a two-step mechanism involving a first TS corresponding to formation of the O(1)−C(2) bond, followed by a second TS associated to the electrocyclic ring closure of the corresponding intermediate, *via* formation of C(3)−C(4) bond (mechanism **B**, Scheme 1). These authors found that the latter mechanism is *ca.* 17 kcal/mol lower in energy than the former. In addition, PPRL found that the stationary points corresponding to mechanism **B** have a very strong biradical character. However, these conclusions may be debatable on two grounds. First, the two-step mechanism proposed by PPRL is very similar to that reported for the reaction between ketenes and imines.[14] According to this mechanism, the torquoelectronic[15] effects which are operating in its second step should induce a high stereocontrol.[16,17] However, according to the experimental evidence available, the stereoselectivity observed in the uncatalyzed reaction between ketenes and carbonyl compounds is in general very poor,[2] Secondly, it is well-known that semiempirical methods tend to overstimate the stability of biradicals,[18] Therefore, it is not clear that the two-step mechanism **B** is of lower energy than the concerted one, if this overestimation factor is taken into account.

As an extension of our previous work and in order to address the questions raised up by the PPRL paper, the objectives of the present work have been to study the [2 + 2] cycloaddition between ketene and formaldehyde using an *ab initio* multiconfigurational level as well as to understand the origin of the stereochemical outcome of the uncatalyzed and catalyzed reaction between asymmetrically substituted ketenes and carbonyl compounds to yield *cis*- and *trans*-2-oxetanones. As model reactants we have chosen chloroketene as a simple monosubstituted activated ketene and acetaldehyde as a model alkyl carbonyl compound. Borane was used to model a computationally tractable Lewis acid. The reactions studied are collected in Scheme 2.

Table 1. Activation Energies (ΔE_a) and Reaction Energies (ΔE_{rxn}) Obtained[a,b] in the Reaction between Ketene **1** and Aldehydes **2a,b** To Form 2-Oxetanones **3**

reaction	TS	level of theory	ΔE_a $\epsilon = 1$	ΔE_a $\epsilon = 9.08$	ΔE_{rxn} $\epsilon = 1$	ΔE_{rxn} $\epsilon = 9.08$
1 + **2a** → *trans*-**3a**	**TS1a**	HF/6-31G*	36.34	32.98	−27.52	−27.72
		MP2/6-31G*	18.47	18.90	−36.50	−36.69
1 + **2a** → *trans*-**3a**	**TS2a**	HF/6-31G*	46.69	46.38	−27.52	−27.72
		MP2/6-31G*	29.67	31.29	−36.50	−36.69
1 + **2a** → *cis*-**3a**	**TS3a**	HF/6-31G*	37.72	37.00	−26.77	−26.90
		MP2/6-31G*	19.20	20.43	−36.19	−36.44
1 + **2a** → *cis*-**3a**	**TS4a**	HF/6-31G*	44.09	42.80	−26.77	−26.90
		MP2/6-31G*	28.34	28.34	−36.19	−36.44
1 + **2b** → *trans*-**3b**	**TS1b**	HF/6-31G*	25.57	29.42	−23.92	−22.10
		MP2/6-31G*	11.81	14.67	−28.15	−30.17
1 + **2b** → *trans*-**3b**	**TS2b**	HF/6-31G*	27.13	29.04	−23.92	−22.10
		MP2/6-31G*	13.63	14.61	−28.15	−30.17
1 + **2b** → *cis*-**3b**	**TS3b**	HF/6-31G*	23.75	30.12	−23.18	−21.19
		MP2/6-31G*	9.75	13.15	−27.86	−29.63
1 + **2b** → *cis*-**3b**	**TS4b**	HF/6-31G*	30.81	30.95	−23.18	−21.19
		MP2/6-31G*	16.79	17.33	−27.86	−29.63

[a] Single-point energies calculated on optimized HF/6-31G* geometries. All the differences in energy are given in kcal/mol, including ZPVE correction, scaled by 0.89 (see text). [b] The values obtained in dichloromethane solution have been computed using the Onsager model.

Computational Methods

All calculations reported in this work have been performed using either GAUSSIAN 92[19] and GAMESS[20] packages, with the 3-21G and 6-31G* basis sets,[21] The TS corresponding to the parent reaction between ketene and formaldehyde to yield 2-oxetanone was fully optimized using the complete active space SCF (CASSCF) approach.[22] All the remaining stationary points have been fully optimized at the HF/6-31G* level of theory, and the energies have been recalculated at the MP2/6-31G* level,[23] keeping the core electrons frozen. Zero-point vibrational energies (ZPVE) calculated at HF/6-31G* level have been scaled[24] by 0.89. Stationary points were characterized by frequency calculations.[25] All reactants and products have positive defined Hessian matrices. TSs showed only one negative eigenvalue in their diagonalized force constant matrices, and their associated eigenvectors were confirmed to correspond to motion along the reaction coordinate. The total energies at HF/6-31G* and MP2/6-31G* levels of all the stationary points included in this work are reported in Table 1 of the supporting information. Energy barriers computed at HF/6-31G*+ΔZPVE and MP2/6-31G*//HF/6-31G*+ΔZPVE levels are collected in Table 1. Unless otherwise stated, all the relative energies discussed in the next section correspond to the MP2/6-31G*//HF/6-31G*+ΔZPVE level. Atomic charges[26] and bond indices[27] were calculated with the natural bonding analysis (NBA) method.[28] The atomic charges of the most relevant atoms or groups at the stationary points included in this work can be found in Table 3 of the supporting information.

Synchronicities[29] (S_y), have been calculated by means of a previously reported formula[9]

(11) Pons, J.-M.; Pommier, A.; Rajzmann, M.; Liotard, D. *J. Mol. Struct. (THEOCHEM)* **1994**, *313*, 361.
(12) Dewar, M. J. S.; Zoebish, E. G.; Healy, E. F.; Stewart, J. J. P. *J. Am.Chem.Soc.* **1985**, *107*, 3902.
(13) Dewar, M. J. S.; Doubleday, C. *J. Am. Chem. Soc.* **1978**, *100*, 4935.
(14) (a) Sordo, J. A.; Gonzalez, J.; Sordo, T. L. *J. Am. Chem. Soc.* **1992**, *114*, 6249. (b) Cossío, F. P.; Ugalde, J. M.; Lopez, X.; Lecea, B. Palomo, C. *J. Am. Chem. Soc.* **1993**, *115*, 995.
(15) Nakamura, K.; Houk, K. N. *J. Org. Chem.* **1995**, *60*, 686, and references therein.
(16) (a) Cossío, F. P.; Arrieta, A.; Lecea, B.; Ugalde, J. M. *J. Am. Chem. Soc.* **1994**, *116*, 2085. (b) Lopez, R.; Sordo, T. L.; Sordo, J. A.; Gonzalez, J. *J. Org. Chem.* **1993**, *58*, 7036.
(17) Georg, G. L.; Ravikumar, V. T. In *The Organic Chemistry of β-Lactams*; Georg, G. L., Ed.; Verlag Chemie: New York, 1993; pp 295−331.
(18) (a) Dewar, M. J. S.; Olivella, S.; Stewart, J. J. P. *J. Am. Chem. Soc.* **1986**, *108*, 5771. (b) Dannenberg, J. J.; Tanaka, K. *J. Am. Chem. Soc.* **1985**, *107*, 671. (c) Dewar, M. J. S.; Jie, C. *J. Am. Chem. Soc.* **1987**, *109*, 5893.
(19) Gaussian 92, Revision C.; Frisch, M. J.; Trucks, G. W.; Head-Gordon, M.; Gill, P. M. W.; Wong, M. W.; Foresman, J. B.; Johnson, B. G.; Schlegel, H. B.; Robb, M. A.; Replogle, E. S.; Gomperts, R.; Andres, J. L.; Raghavachari, K.; Binkley, J. S.; Gonzalez, C.; Martin, R. L.; Fox, D. J.; Defrees, D. J.; Baker, J.; Stewart, J. J. P.; Pople, J. A. Gaussian, Inc.: Pittsburgh, PA, 1992.
(20) GAMESS (General Atomic and Molecular Electronic Structure System, CRAY-UNICOS Version). (a) Schmidt, M. W.; Baldridge, K. K.; Boatz, J. A.; Jensen, J. M.; Koseki, S.; Gordon, M. S.; Nguyen, K. A.; Windus, T. L.; Elbert, S. T. *QCPE Bull.* **1990**, *10*, 52. (b) Schmidt, M. W.; Baldridge, K. K.; Boatz, J. A.; Gordon, M. S.; Jensen, J. M.; Koseki, S.; Matsunaga, N.; Nguyen, K. A.; Su, S.; Windus, T. L. *J. Comput. Chem.* **1993**, *14*, 1347.
(21) Hehre, W. J.; Radom, L.; Schleyer, P. v. R.; Pople, J. A. *Ab Initio Molecular Orbital Theory* Wiley; New York, 1986; pp 65−88, and references therein.
(22) Roos, B. O.; Taylor, P. R.; Siegbahn, P. E. M. *Chem. Phys.* **1980**, *48*, 157.
(23) (a) Binkley, J. S.; Pople, J. A. *Int. J. Quantum Chem.* **1975**, *9*, 229. (b) Pople, J. A.; Binkley, J. S.; Seeger, R. *Int. J. Quantum Chem. Symp.* **1976**, *10*, 1.
(24) Pople, J. A.; Schlegel, B.; Krishnan, R.; DeFrees, D. J.; Binkley, J. S.; Frisch, H.; Whiteside, R.; Hout, R. F., Jr.; Hehre, W. J. *Int. J. Quantum Chem. Symp.* **1981**, *15*, 269.
(25) McIver, J. W. Komornicki, A. K. *J. Am. Chem. Soc.* **1972**, *94*, 2625.
(26) Wiberg, K. B.; Rablen, P. R. *J. Comput. Chem.* **1993**, *14*, 1504.
(27) Wiberg, K. B. *Tetrahedron* **1968**, *24*, 1083.

$$S_y = 1 - \frac{\sum_{i=1}^{n} \frac{|\delta B_i - \delta B_{av}|}{\delta B_{av}}}{2n - 2} \quad (1)$$

which is based upon the definition of asynchronicity proposed by Pericàs and Moyano.[29] In eq 1, n is the number of bonds directly involved in the reaction, and the relative variation of bond index (δB_i) for a bond (i) at the TS is given by the following expression:[29]

$$\delta B_i = \frac{B_i^{TS} - B_i^{R}}{B_i^{P} - B_i^{R}} \quad (2)$$

where the superscripts R and P refer to the reactants and the product, respectively. The average value[29] of δB_i, denoted by δB_{av} is therefore

$$\delta B_{av} = n^{-1} \sum_{i=1}^{n} \delta B_i \quad (3)$$

The values of the synchronicities and related magnitudes obtained for the reactions considered in this work are included in Table 2.

Solvent effects have been partially taken into account by means of the self-consistent reaction field (SCRF) method,[30] given the nonspecific interactions between the solute and the solvent in this particular reaction. In our previous paper,[9] we have shown that the relatively simple Onsager model,[31] as implemented in GAUSSIAN 92,[32] provides a satisfactory description of the main variables which are operating in this reaction. In particular, the results provided by this method are comparable to those obtained using a more complete treatment such as the Rinaldi−Rivail method.[33] Therefore, all the SCRF calculations reported in this work have been obtained using the former model. The considered solvent is dichloromethane, a very common one for this kind of reactions. Dichloromethane has a moderately low dielectric constant, namely $\epsilon = 9.08$, which makes the theoretical approach more reliable than for high ϵ solvents. The total energies at the HF(SCRF)/6-31G* and MP2(SCRF)/6-31G* levels, including the spherical cavity radii, obtained from HF/6-31G* wave functions are collected in Table 1 of the supporting information. The relative energies at the HF(SCRF)/6-31G* and MP2(SCRF)/6-31G* levels are included in Table 1.

Results and Discussion

Uncatalyzed Reactions. We started our study exploring the potential energy hypersurface associated to the reaction between ketene and formaldehyde to yield 2-oxetanone, using a CASSCF[22] treatment in order to find out whether the reaction profile of the parent reaction is different at the multiconfigurational level to that reported by us at the RHF level. In order to allow for enough flexibility, we included in the active space six electrons and six orbitals. The orbitals included in the active window were obtained from a single point calculation of the reactants separated by 6 Å. The π-MOs were selected, thus the active space was formed by the $1b_1$ and $2b_1$ MOs of formaldehyde, and by the $2b_2$, $2b_1$, $3b_2$ and $3b_1$ MOs of ketene.[34] This active space generated 175 configuration state functions

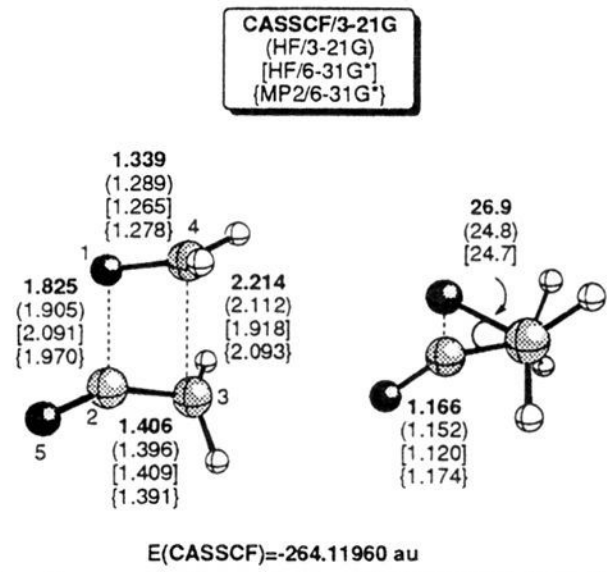

Figure 1. Computer plots of the CASSCF(6,6)/3-21G transition structure corresponding to the [2 + 2] cycloaddition reaction between ketene and formaldehyde to yield 2-oxetanone. Structural data obtained at other computational levels are also shown for comparison. The HF/6-31G* and MP2/6-31G* data are taken from refs 9 and 8, respectively (see text). Bond distances and angles are given in Å and deg, respectively. Dihedral angles are given in absolute value. In this and all the remaining figures which include ball-and-stick representations, unless otherwise stated, atoms are represented by increasing order of shadowing as follows: H, C, and O.

(CSFs). Given the size of the calculation, the 3-21G basis set was used in this case. Intensive search[35] along the CASSCF(6,6)/3-21G potential energy hypersurface led to the location of a TS, whose chief geometrical features are shown in Figure 1. As it can be seen, this TS corresponds to a concerted $[\pi 2_s + (\pi 2_s + \pi 2_s)]$ mechanism, whose geometry is very similar to that found at RHF/3-21G level (see Figure 1). This TS has C_1 symmetry, with a dihedral angle between the C(2), O(1), C(4) and C(3) atoms of 26.9° (the value at HF/3-21G level is 24.8°). Interestingly, the distance between O(1) and C(2) is shorter than that corresponding to the C(3)−C(4) bond in formation, both at CASSCF(6,6)/3-21G and RHF/3-21G levels (see Figure 1). In our previous work[9] we found that at RHF/6-31G* level the relative order of lengths is reversed, whereas Yamabe *et al.*[8] have reported a TS computed at MP2/6-31G* level which is closer to our CASSCF geometry (see Figure 1). Therefore, the relative lengths of the new forming σ bonds vary from one theoretical level to another and do not determine alternative mechanisms, as it was suggested in the PPRL paper. In order to assess the biradical character of the TS reported in Figure 1, we focused our attention to the CASSCF(6,6) wave function obtained. Among the 175 CSFs generated, only four contributed to the total wave function with a weight higher to 1%. These CSFs have been collected in Table 2 of the supporting information. Inspection of the data included in such a table reveals that the CSF associated to the closed-shell S_o wave function is largely the predominant one, with a coefficient of 0.933. In addition, the occupancies of the corresponding three

Table 2. Bond Indices[a,b] of TSs and Synchronicities[a,c] (S_y) Obtained for the Reaction between Ketene **1** and Aldehydes **2a,b** To Yield 2-Oxetanones *cis*- and *trans*-**3a,b**

	B_{12}		B_{23}		B_{34}		B_{14}		δB_{av}		S_y	
TS	$\epsilon = 1$	$\epsilon = 9.08$	$\epsilon = 1$	$\epsilon = 9.08$	$\epsilon = 1$	$\epsilon = 9.08$	$\epsilon = 1$	$\epsilon = 9.08$	$\epsilon = 1$	$\epsilon = 9.08$	$\epsilon = 1$	$\epsilon = 9.08$
TS1a	0.453	0.596	1.347	1.380	0.263	0.213	1.308	1.275	0.432	0.449	0.874	0.814
TS2a	0.465	0.566	1.355	1.379	0.246	0.217	1.256	1.216	0.442	0.458	0.858	0.809
TS3a	0.350	0.483	1.322	1.383	0.312	0.231	1.291	1.270	0.430	0.466	0.857	0.806
TS4a	0.629	0.681	1.311	1.302	0.271	0.278	1.246	1.205	0.505	0.530	0.850	0.846
TS1b	0.012	0.010	1.225	1.264	0.495	0.445	1.204	1.211	0.425	0.388	0.676	0.675
TS2b	0.012	0.010	1.209	1.256	0.506	0.449	1.204	1.212	0.433	0.391	0.676	0.674
TS3b	0.013	0.028	1.219	1.299	0.526	0.451	1.175	1.187	0.444	0.386	0.676	0.683
TS4b	0.011	0.010	1.194	1.208	0.520	0.529	1.188	1.176	0.447	0.440	0.675	0.674

[a] Properties computed from RHF/6-31G* wave functions. [b] Natural localized molecular orbital bond indices. [c] Synchronicities calculated from eqs 1−3 (see text). [d] The quantities obtained in dichloromethane solution ($\epsilon = 9.08$) have been computed using the Onsager model.

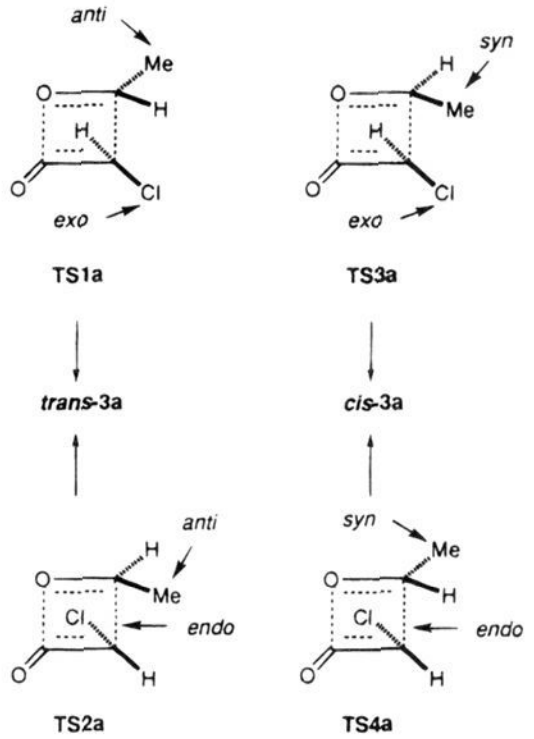

Figure 2. Schematic representation of the possible interaction modes between chloroketene **1** and acetaldehyde **2a** to form β-lactones ***cis***- and ***trans*-3a**.

lowest energy natural orbitals are very close to 2.0, whereas the occupancies of the remaining three natural orbitals is almost negligible. Therefore, we can conclude that the TS corresponding to the parent reaction is described adequately with a single reference wave function.

The next step in our study has been to elucidate the origins of the stereochemical outcome of the uncatalyzed reaction. In order to achieve this goal, we selected chloroketene **1**, a model activated (i.e., electrophilic) ketene, and acetaldehyde **2a**, a model unsymmetrically substituted carbonyl compound as reactants. In principle, the possible cycloadducts which can be obtained from these reactants are *cis*- and *trans*-3-chloro-4-methyl-2-oxetanone **3a** (see Scheme 2). Since the $[_\pi 2_s + (_\pi 2_s + _\pi 2_s)]$ geometry of the corresponding TSs imposes a torsion around the C(2)−C(3) bond of the ketene subunit, the chlorine atom can be either in an *exo* or *endo* disposition with respect to the ring in formation. On the other hand, the methyl group at C(4) can be in a *syn* or *anti* disposition with respect to the chlorine atom at C(3). These possible geometries generate a total of four alternative transition structures **TS1a**−**TS4a**, depicted in Figure 2. According to the stereochemical relationships present in these TSs, **TS1a** and **TS2a** should lead to *trans*-**3a**, whereas *cis*-**3a** can be formed *via* either **TS3a** or **TS4a**. We have located and characterized these four TSs on the HF/6-31G* potential energy hypersurface corresponding to the [2 + 2] cycloaddition

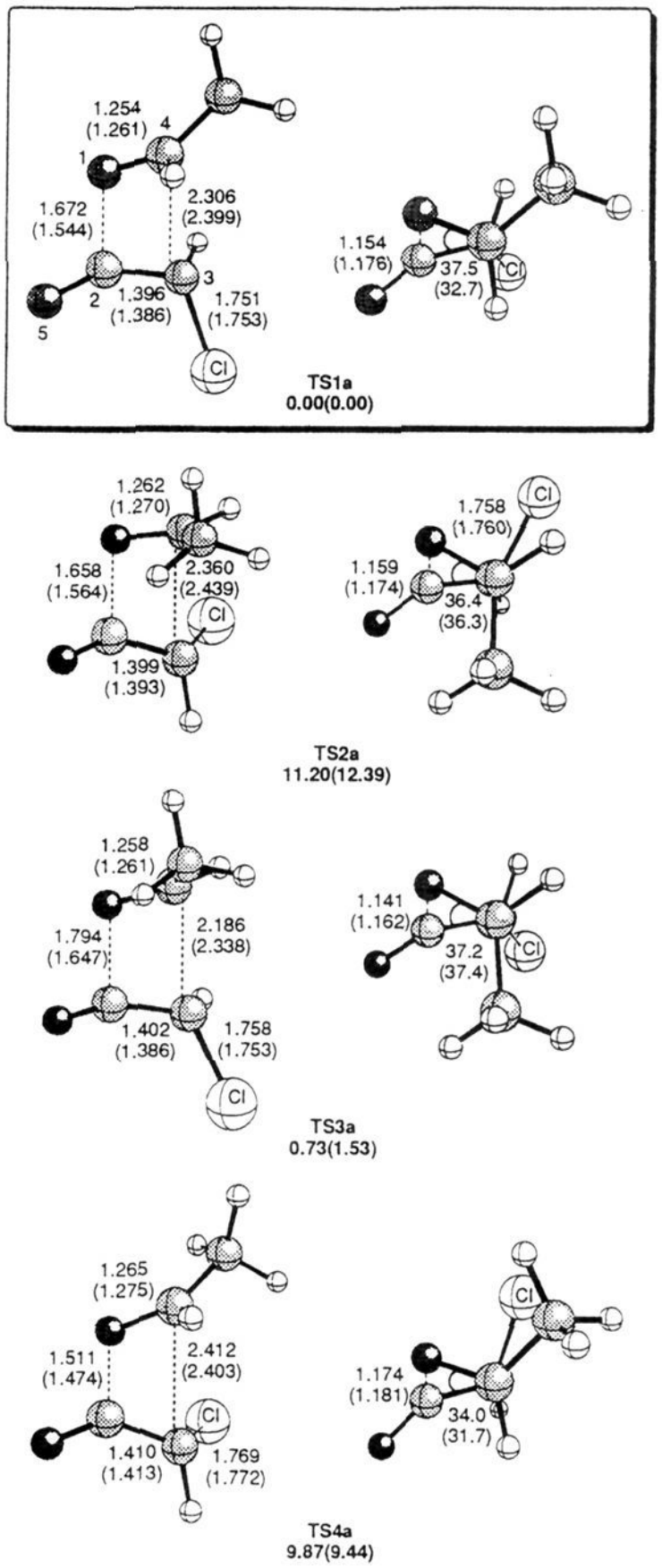

Figure 3. HF/6-31G* and HF(SCRF)/6-31G* (in parentheses) optimized geometries of transition structures **TS1**-**4a**. Bond distances and angles are given in Å and deg, respectively. Dihedral angles are given in absolute value. Bold numbers are the relative energies in kcal/mol at MP2/6-31G*//HF/6-31G*+ΔZPVE level.

between **1** and **2a** to yield either *cis* and *trans*-**3a**. The main geometrical features of these TSs are depicted in Figure 3. In all four saddle points, the O(1)−C(2) bond distances are shorter than the C(3)−C(4) bond distances. Thus, in the gas phase the former distances lie in the 1.511−1.794 Å interval, whereas the latter vary from 2.186 to 2.412 Å (see Figure 3). These

(28) (a) Reed, A. E.; Weinstock, R. B.; Weinhold, F. *J. Chem. Phys.* **1995**, *83*, 735. (b) Reed, A. E.; Curtiss, L. A.; Weinhold, F. *Chem. Rev.* **1988**, *88*, 899. (c) Reed, A. E.; von Ragué Schleyer, P. *J. Am. Chem. Soc.* **1990**, *112*, 1434.

(29) Moyano, A.; Pericàs, M. A.; Valentí, E. *J. Org. Chem.* **1989**, *54*, 573.

(30) (a) Tomasi, J.; Persico, M. *Chem. Rev.* **1994**, *94*, 2027. (b) Minkin, V. I.; Simikin, B. Ya.; Minyaev, R. M. *Quantum Chemistry of Organic Compounds*; Springer Verlag: Berlin, 1990; pp 88−105. (c) Simikin, B. Ya.; Sheikhet, I. I. *Quantum Chemical and Statistical Theory of Solutions-A Computational Approach*; Ellis Horwood: London, 1995; pp 40−103.

(31) Onsager, L. *J. Am. Chem. Soc.* **1936**, *58*, 1486.

(32) Wong, M. W.; Frisch, M. J.; Wiberg, K. B. *J. Am. Chem. Soc.* **1991**, *113*, 4776.

(33) (a) Rinaldi, D.; Rivail, J. L.; Rguini, N. *J. Comput. Chem.* **1992**, *13*, 675. (b) Rinaldi, D. *J. Comput. Chem.* **1982**, *6*, 155. (c) Rinaldi, D.; Ruiz-López, M. F.; Rivail, J. L. *J. Chem. Phys.* **1983**, *78*, 834. (c) Rivail, J. L.; Rinaldi, D.; Ruiz-López, M. F. In *Theoretical and Computational Models for Organic Chemistry*; Formosinho, S. J., Csizmadia, I. G., Arnaut, L., Eds.; Kluwer Academic Publishers: Dordrecht, 1991; NATO ASI Series C, Vol. 339, pp 79−92. (d) Rivail, J. L. In *New Theoretical Concepts for Understanding Organic Reactions*; Bertrán, J., Csizmadia, I. G., Eds.; Kluwer Academic Publishers: Dordrecht, 1989; NATO ASI Series C, Vol. 267, pp 219−229.

(34) Hout, R. F.; Pietro, W. J.; Hehre, W. J. *A Pictorial Approach to Molecular Structure and Reactivity*; Wiley: New York, 1984; pp 169−170 and 208−209.

(35) We tried to locate the stationary point corresponding to the path B depicted in Scheme 1. All our attempts using CASSCF/3-21G and GVB/3-21G wave functions were unfruitful. In particular, the hypothetical intermediate present in the mechanism B converged to the separate reactants upon optimization. Similarly, the second TS of Path B converged to the TS corresponding to path A (see Figure 1).

(36) Shambayati, S.; Schreiber, S. L. In *Comprehensive Organic Synthesis*; Trost, B. M., Fleming, I., Eds.; Pergamon: Oxford, 1991; Vol. 5, pp 283−324.

values correspond to bond order intervals for B_{12} and B_{34} of 0.629−0.350 and 0.246−0.312, respectively (see Table 2). These results can be explained in terms of the high electrophilicity of chloroketene **1**, induced by the electron-withdrawing chlorine atom. This favors the nucleophilic addition of the oxygen atom of acetaldehyde over the *sp* hybridized atom of chloroketene, whereas interaction between C(3) and C(4) atoms is developed into a lesser extent because of the poor overlap between the *p*-AOs located on these atoms. The noncoplanar interaction between **1** and **2a** is evidenced in the Newman projections of **TS1a**−**TS4a** depicted in Figure 3. The absolute values of the dihedral angles ω = O(1)−C(4)···C(3)−C(2) vary slightly from one TS to another, their values ranging from 31.7° to 37.5°. All these data indicate that the four TSs found for the interaction between **1** and **2a** correspond to the $[_{\pi}2_s+(_{\pi}2_s+_{\pi}2_s)]$ mechanism, in which **TS1a**−**TS4a** are almost "halfway" between reactants and products (δB_{av} vary from 0.442 to 0.505) and are relatively synchronous, the computed values of S_y being between 0.850 and 0.874. Our calculations also indicate that the solvent induces an additional asynchronous character in all the saddle points **TS1a**−**TS4a**. Thus, the O(1)−C(2) bonds are more advanced than in the gas phase, the bond distances being in the range 1.474−1.647 Å (The corresponding bond indices B_{12} vary from 0.681 to 0.483). Similarly, the C(3)−C(4) bonds are developed into a lesser extent than those of the gas phase, with the exception of **TS4a**. The bond distances between these atoms are in the range 2.338−2.403 Å, the B_{34} values varying from 0.213 to 0.278. The calculated synchronicities at HF(SCRF)/6-31G* level are slightly lower than those found *in vacuo* (see Table 2), the average difference between both values being of *ca.* 0.04.

The main geometrical and, especially, energetic difference between the four TSs are determined by the *exo* or *endo* disposition of the chlorine atom at C(3). Thus, **TS1a**, is 11.20 kcal/mol more stable than **TS2a** in the gas phase, both TSs corresponding to the formation of the same [2 + 2] cycloadduct *trans*-**3a**. Similarly, **TS3a**, which has a 3-*exo* chlorine atom, is 9.14 kcal/mol more stable in vacuo than its 3-*endo* analog **TS4a**, both TSs leading to *cis*-**3a**. The lower energy of the 3-e*xo* saddle points can be explained in terms of the steric congestion present in the *endo* TSs, along with the electrostatic repulsion between the O(1) and 3-Cl atoms. Thus, the NBA charges for O(1) vary from −0.623e to −0.730e (gas phase data, see Table 3 of the supporting information), and the charges of the chlorine atom are −0.041e and −0.074e for **TS2a** and **TS4a**, respectively. Therefore, the two possible 3-*exo* saddle points **TS1a** and **TS3a**, leading to *trans*-**3a** and *cis*-**3a**, respectively, correspond to the more likely reaction paths. **TS3a** is slightly more energetic than **TS1a** (0.73 kcal/mol in the gas phase, see Figure 3) because of the proximity between the substituents at C(3) and C(4). The difference in energy between both TSs is increased in solution. As a consequence, preferential formation of the cycloadduct *trans*-**3a** is predicted both in the gas phase and in solution. The lowest activation energies corresponding to the **1**+**2a** → *trans*-**3a** process *via* **TS1a** are 18.47 and18.90 kcal/mol *in vacuo* and in solution, respectively (see Table 1). In this case, the lowest energies of activation are concomitant with the highest reaction energies (−36.50 and−36.69 kcal/mol *in vacuo* and in solution respectively, see Table 1). This should be expected, since *trans*-**3a** is predicted to be more stable than *cis*-**3a**, in which the substituents at C(3) and C(4) are on opposite sides of the molecular plane (see Figure 7). Therefore, preferential formation of the *trans* cycloadducts is predicted under both kinetic and thermodynamic control, although the kinetic stereoselection is not very pronounced, specially in the gas phase.

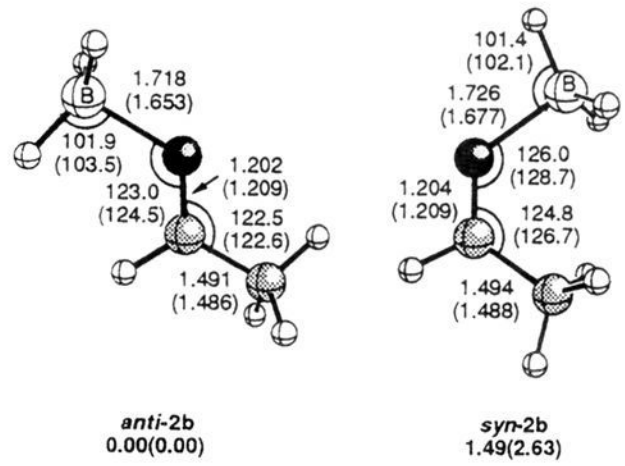

Figure 4. HF/6-31G* and HF(SCRF)/6-31G* (in parentheses) optimized geometries of structures **2b**. Bond distances and angles are given in Å and deg respectively. Bold numbers are the relative energies in kcal/mol at MP2/6-31G*//HF/6-31G*+ΔZPVE level.

Catalyzed Reactions. We have also explored the potential energy surface corresponding to the interaction between chloroketene **1** and the acetaldehyde−borane complex. In principle, two possible complexes **2b** can be formed, assuming a nonlinear coordination between boron and the carbonyl group.[36] We have located two stereoisomers for **2b**, which are depicted in Figure 4. The *anti*-**2b** adduct is calculated to be 1.49 kcal/mol more stable than its *syn* stereoisomer in the gas phase, the corresponding value in dichloromethane solution being 2.63 kcal/mol. These results are qualitatively in agreement with the experimental evidence available[36] and with previous suggestions made by different authors.[7,37] The preference for the *anti* complex is increased when solvent effects are taken into account. In addition, the interaction between the boron atom and one of the lone pairs of acetaldehyde is calculated to be stronger at the HF(SCRF)/6-31G* level. Thus, the B−O bond distances for *anti*-**2b** are 1.718 and 1.653 Å in the gas phase and in solution, respectively. This shrinkage parallels a relative elongation in the bond distance of the carbonyl group (see Figure 4). These results are compatible with a significant zwitterionic character of the complexes **2b**, since bonding between borane and acetaldehyde implies the development of a negative charge in the borane moiety at the expenses of the oxygen atom. Thus, the NBA charge of the borane subunit in *anti*-**2b** are −0.214e and −0.251e, *in vacuo* and in solution, respectively (see Table 3 of the supporting information). The electrostatic interaction between the solvent and the dipole associated to this partial charge separation contributes to the additional stabilization of *anti*-**2b**. On the other hand, the destabilizing interaction between the BH_3 and methyl groups in *syn*-**2b** is enhanced by the shorter B−O distances in solution. This destabilization cannot be completely alleviated by the relatively higher B−O bond distances in *syn*-**2b** and higher B−O−C and O−C−C bond angles (see Figure 4).

After considering the possible interaction modes between both isomers of **2b** and chloroketene **1**, the approaching geometries depicted in Figure 5 are obtained.[38] According to this scheme, *syn*-**2b** can generate two transition structures, denoted as **TS1b** and **TS4b** in Figure 5, in which the chlorine atom and the methyl group are in a 3,4-*anti* and 3,4-*syn* relationship, respectively. Similarly, interaction between *anti*-**2b** and **1** can take place through the transition structures **TS2b** and **TS3b**, in which the groups at C(3) and C(4) are 3,4-*anti* and 3,4-*syn* each other, respectively. Therefore, **TS1b** and **TS2b** correspond to the formation of *trans*-**3b**, whereas *cis*-**3b** can be formed either via **TS3b** or **TS4b**.

(37) See, for example: (a) Corey, E. J.; Sarshar, S.; Bordner, J. *J. Am. Chem. Soc.* **1992**, *114*, 7938. (b) Nevalainen, V. *Tetrahedron Asymmetry* **1993**, *4*, 2517.

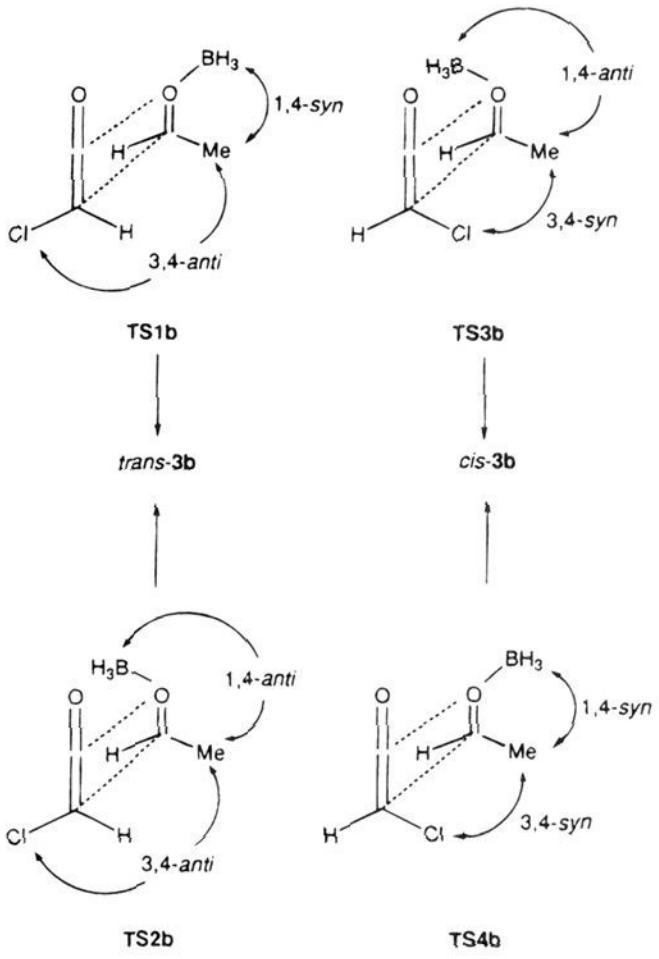

Figure 5. Schematic representation of the possible interaction modes between the chloroketene **1** and the BH_3−acetaldehyde complex **2b** to form the β-lactones ***cis*** and ***trans*-3b**.

We have located and characterized the four saddle points **TS1−4b** on both the HF/6-31G* and HF(SCRF)/6-31G* potential energy hypersurfaces. The chief geometrical features of these TSs are shown in Figure 6. All these saddle points exhibit some similar characteristics.

Thus, bonding between C(3) and C(4) is very advanced, whereas the O(1)−C(2) bonds are only slightly developed, both in the gas phase and in solution (see Table 2). This latter feature is responsible for the relatively low synchronicities with respect to the uncatalyzed processes. These synchronicities do not vary significantly when solvent effects are included, the average value of S_y being 0.676. Also it should be pointed out that **TS1−4b** transition structures have zwitterionic character, the acetaldehyde−borane subunit possessing an average charge of *ca.* −0.4e, at the expense of the ketene fragment, both in the gas phase and in solution (see Table 3 of the supporting information). Although the above mentioned characteristics of these TSs are not significantly affected by solvent effects, the *relative* energies between the different diastereomeric saddle points and the dihedral angles ω = O(1)−C(4)···C(3)−C(2) do vary appreciably when solvent effects are considered. We shall comment first on results obtained in the gas phase.

(38) It should be taken into account that the catalyzed reaction does not correspond to a $[_\pi 2_s + (_\pi 2_s + _\pi 2_s)]$ mechanism, but to a two-stage process in which bond formation between C(3) and C(4) is much more advanced than in the uncatalyzed reaction (see ref 9). As a consequence, the *endo* and *exo* positions become equivalent in the catalyzed reaction. This situation can be visualized by means of the following diagram:

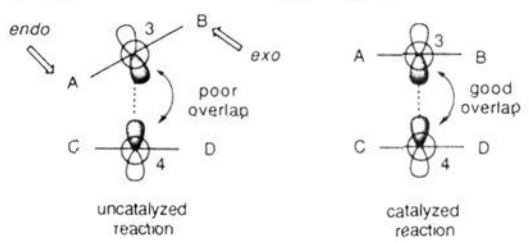

In fact, when the four TSs depicted in Figure 3 where submitted to optimization including a BH_3 group coordinated to the O(1) atom, only four non-equivalent TSs where obtained (*vide infra*).

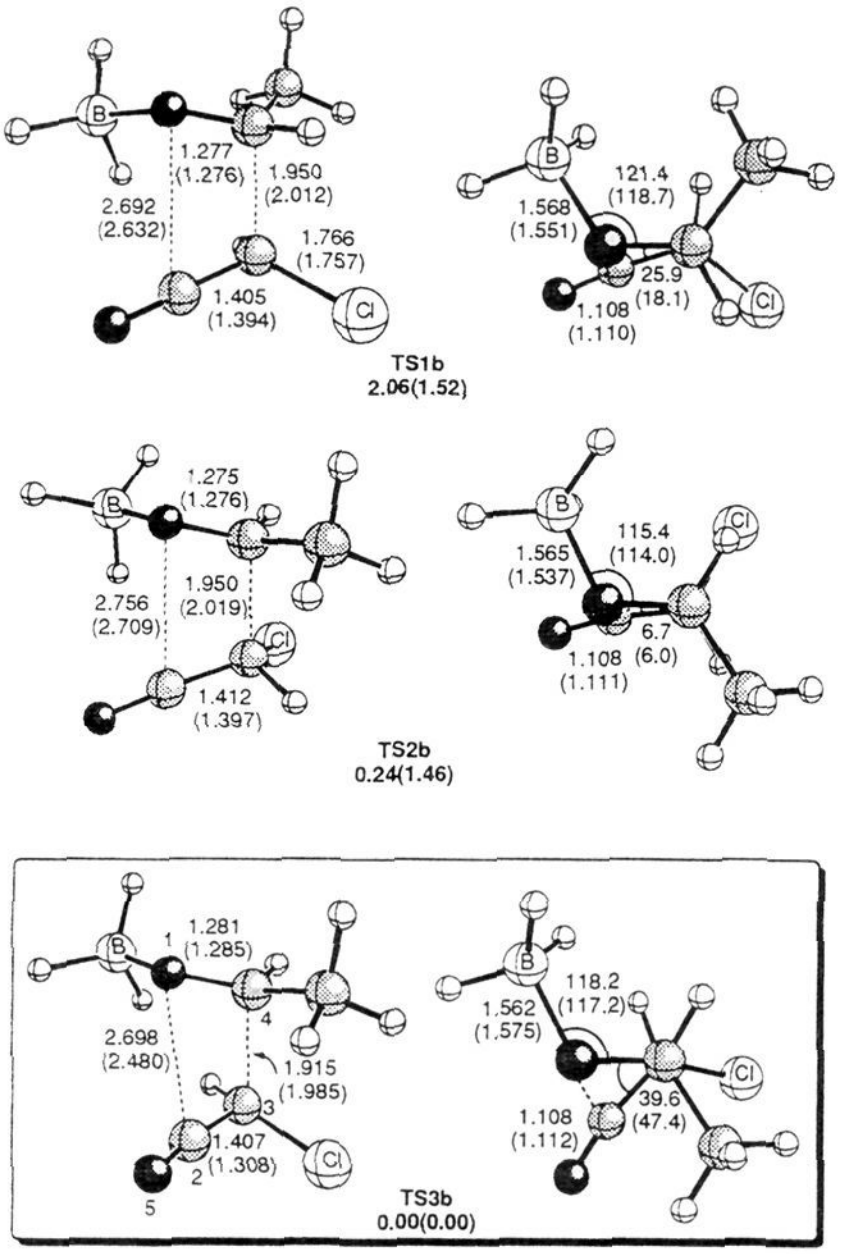

Figure 6. HF/6-31G* and HF(SCRF)/6-31G* (in parentheses) optimized geometries of transition structures **TS1-4b**. Bond distances and angles are given in Å and deg. respectively. Dihedral angles are given in absolute value. Bold numbers are the relative energies in kcal/mol at MP2/6-31G*//HF/6-31G*+ΔZPVE level.

The order of energies for the TSs obtained *in vacuo* is the following: **TS3b** < **TS2b** < **TS1b** < **TS4b** (see Table 1 of the supporting information and Figure 6). As it should be expected on the basis of the relative stabilities of *syn*-**2b** and *anti*-**2b**, the saddle points having a 1,4-*anti* relationship between the borane and methyl groups (**TS2b** and **TS3b**) are of lower energy than their 1,4-*syn* analogues (**TS1b** and **TS4b** respectively, see Figure 6). Accordingly, the former saddle points differ in the relative orientation of the substituents at C(3) and C(4). Our calculations in the gas phase indicate that **TS2b** is almost isoenergetic to **TS3b**, the difference in energy between them being of only 0.24 kcal/mol. This agrees with the available experimental evidence, since it is known that the catalyzed reaction between ketenes and carbonyl compounds takes place with poor stereocontrol, although the *cis* cycloadducts are slightly predominant.[2]

The relative stabilities of the four TSs of the catalyzed

reaction are somewhat different in solution, and the sequence is now **TS3b** < **TS4b** < **TS2b** < **TS1b**. Thus, the difference in energy between **TS3b** and **TS4b**, both of them leading to the formation of *cis*-**3b**, is 1.24 kcal/mol, whereas in the gas phase it is 2.92 kcal/mol (see Figure 6). This relative stabilization can be explained by the relative orientation of the dipoles associated to the O(1)−B and C(3)−Cl bonds in both TSs, readily appreciated in the Newman projections depicted in Figure 6. According to this, since the dipole moment of **TS4b** is higher than that of **TS3b** (3.773 D and 3.070 D at HF(SCRF)/6-31G* level) the stabilizing electrostatic solute-solvent interaction is higher in **TS4b**, thus resulting in a lower energy gap between both TSs. The almost isoenergetic relationship between **TS1b** and **TS2b** in solution can be explained on the same basis, the respective calculated dipole moments being 2.835 and 3.388 D, respectively. The relative destabilization of **TS2b** with respect to **TS3b** in solution (1.46 *vs* 0.24 kcal/mol in the gas phase, *vide supra*) can be accounted for considering that the bond distances between the boron atom and O(1) are shorter in solution (see Figure 6). This results in a higher destabilizing interaction between the catalyst and the chlorine atom in **TS2b**. The low value of ω in this TS partially alleviates this repulsion, but at the cost of increasing the eclipsing of the whole structure (see the Newman projection of **TS2b** in Figure 6). By contrast, **TS3b** adopts a staggered conformation, the absolute value of its dihedral angle ω being 47.4° in solution. Hence, since **TS3b** is again the saddle point of lower energy, preferential formation of *cis*-**3b** is also predicted in solution.

The lowest activation energies found for the catalyzed reaction *anti*-**2b**+**1** → *cis*-**3b** are 9.75 and 13.15 kcal/mol *in vacuo* and in solution, respectively. This supposes a descent in activation energy with respect to the uncatalyzed reaction of 8.72 and 5.75 kcal/mol, respectively (see Table 1). The corresponding reaction energies for $\epsilon = 1$ and $\epsilon = 9.08$ are −27.86 and−29.63 kcal/mol. It is important to note that the reaction energies for the catalyzed processes are lower than those found in the preceding section. This particular aspect will be discussed later. The structures of *cis*- and *trans*-**3b** corresponding to complexation of the borane with *cis*- and *trans*-**3a** *via* the oxygen atom of the carbonyl group[39] are depicted in Figure 7. As we have found previously,[9] inclusion of solvent effects induces a considerable shortening in the B−O(5) bond distances (ca. 0.5 Å, see Figure 7), which demonstrates the importance of solvent effects for the Lewis acid complexation of carbonyl compounds. This shortening in the B-O(5) distance induces an enlargement of the C(2)−O(5) distance and a shortening of the O(1)−C(2) distance. A more noteworthy point is that the differences in energy between the *cis* and *trans* complexes **3b** are considerably smaller than those found for the uncomplexed 2-oxetanones **3a**, both in the gas phase and in solution, nevertheless *trans*-**3b** is again a bit more stable.

In order to explore computationally the efficiency of the catalyst turnover, we have considered the isodesmic equation shown in Scheme 3. The ΔE value for this equation indicates the substrate affinity of the catalyst and conversely reflects the degree of product inhibition. The ΔE values obtained at the HF/6-31G*+ΔZPVE and MP2/6-31G*//HF/6-31G*+ΔZPVE levels, both in the gas phase and in solution, are reported in Table 3. Notice that the values of ΔE are higher in the case of the *cis*- and *trans*-3-chloro-4-methyl-2-oxetanones than in the case of the whole unsubstituted 2-oxetanone. Another interesting point is that the values of ΔE are significantly affected by both electron correlation and solvent effects. This provides further evidence of the importance of these phenomena in Lewis acid complexation processes.[36] Nevertheless, for the substituted cases the ΔE values are high enough to ensure the efficiency of the catalytic cycle.

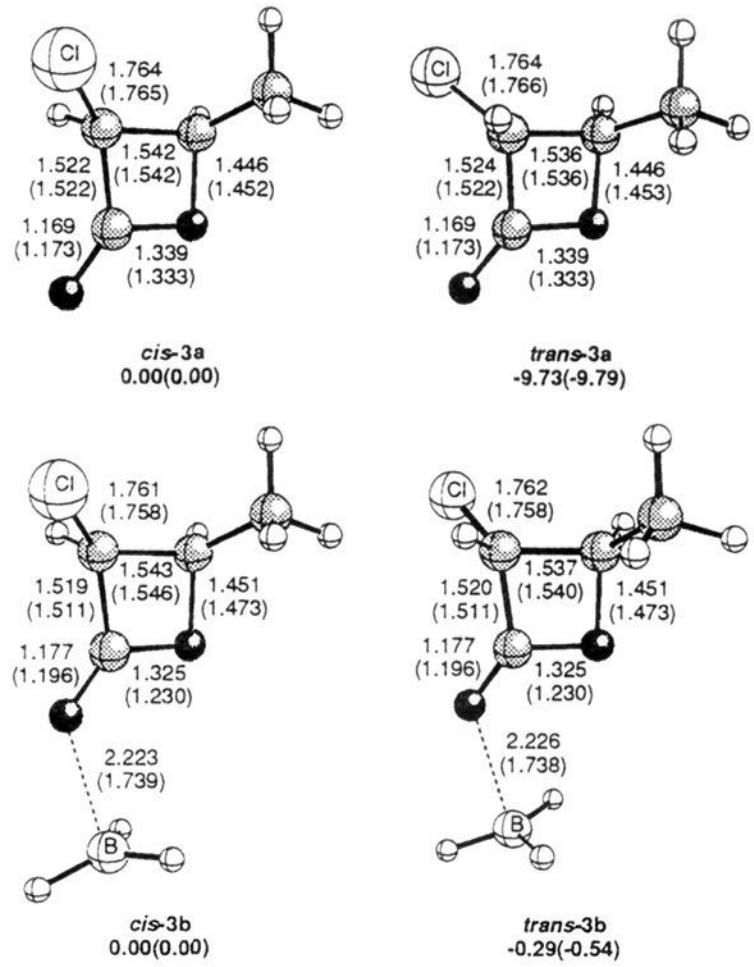

Figure 7. HF/6-31G* and HF(SCRF)/6-31G* (in parentheses) optimized geometries of 2-oxetanones ***cis***- and ***trans*-3a,b**. Bond distances and angles are given in Å and deg, respectively. Bold numbers are the relative energies in kcal/mol at MP2/6-31G*//HF/6-31G*+ΔZPVE level.

Scheme 3

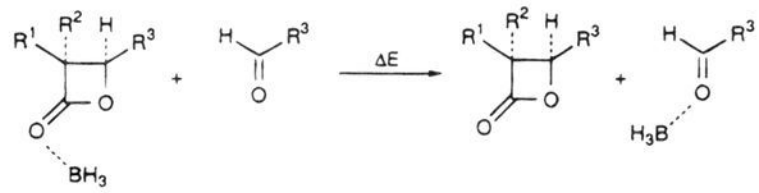

Table 3. Energies[a,b] (ΔE, kcal/mol) Corresponding to the Isodesmic Equation Represented in Scheme 3

				ΔE(HF/6-31G*)		ΔE(MP2//6-31G*)	
entry	R^1	R^2	R^3	$\epsilon = 1.0$	$\epsilon = 9.08$	$\epsilon = 1.0$	$\epsilon = 9.08$
1[c]	H	H	H	−1.16	+0.62	−2.98	−0.26
2	Cl	H	Me	−3.68	−5.71	−8.42	−6.81
3	H	Cl	Me	−3.60	−5.62	−8.44	−6.52

[a] Single point energies calculated on HF/6-31G* fully optimized geometries. [b] Zero-point vibrational energies, scaled by 0.89, are included. [c] Data taken from ref 9.

Conclusions. The following conclusions can be drawn from the *ab initio* calculations included in this work: (i) The uncatalyzed reaction between ketenes and carbonyl compounds takes place *via* $[{}_{\pi}2_s+({}_{\pi}2_s+{}_{\pi}2_s)]$ transition structures which display closed-shell character and therefore can be conveniently described within the Hartree−Fock formalism. (ii) The stereocontrol of the uncatalyzed [2 + 2] cycloaddition between monosubstituted activated ketenes and aldehydes is oriented toward preferential formation of the corresponding *trans*-cycloadducts. (iii) In the case of Lewis acid catalyzed reactions, much more significant from a synthetic standpoint, formation of *cis*-2-oxetanones is favored. This stereochemical outcome

(39) As we have previously reported, the complexes in which the Lewis acid catalyst is bound to the O(1) atom are less stable than *cis*- and *trans*-**3b**. See ref 9.

(40) For a recent example on the improvement of the *cis-trans* diastereoselection by means of bulky Lewis acid catalyst, see: Maruoka, K.; Concepcion, A.-B.; Yamamoto, H. *Synlett.* **1992**, 31.

takes place through transition structures whose favored geometry is;

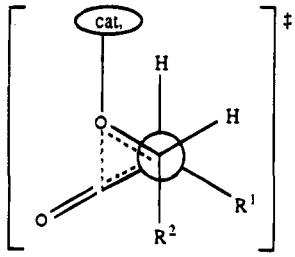

This model is determined by the *anti* coordination of the catalyst to the oxygen of the carbonyl compound and the staggered conformation around the C(3)···C(4) bond in formation. According to our model, the more bulky the catalyst is, the higher the stereocontrol, in agreement with the experimentally available evidence.[2,40] (iv) The catalyzed reaction is not affected by product inhibition. However, in order to obtain accurate enough results for the reaction profile of these reactions, both electron correlation and solvent effects must be taken into account.

Acknowledgment. This work has been supported by the Universidad del País Vasco-Euskal Herriko Unibertsitatea (Project UPV 170.215-EA156/94), by the Gobierno Vasco-Eusko Jaurlaritza (Project GV 170.215-0119/94), and by Diputación Foral de Gipuzkoa-Gipuzkoako Foru Aldundia (Project 0733/94). We thank the Plan Nacional de I+D (Comisión Interministerial de Ciencia y Tecnología) and the CIEMAT for a generous gift of computing time at the CRAY YMP-EL computer.

Supporting Information Available: Cartesian coordinates of all the structures discussed in the text and tables including total energies, zero-point vibrational energies and spherical cavity radii; configuration state functions and related parameters associated to the transition structure depicted in Figure 1; NBA charges of the stationary points discussed in the text (14 pages). This material is contained in many libraries on microfiche, immediately follows this article in the microfilm version of the journal, can be ordered from the ACS, and can be downloaded from the Internet; see any current masthead page for odering information and Internet access instructions.

JA951750P